Band structure of the one-dimensional metallic (SN) x crystal

A. Zunger

Citation: The Journal of Chemical Physics **63**, 4854 (1975); doi: 10.1063/1.431228
View online: http://dx.doi.org/10.1063/1.431228
View Table of Contents: http://scitation.aip.org/content/aip/journal/jcp/63/11?ver=pdfcov
Published by the AIP Publishing

Band structure of the one-dimensional metallic $(SN)_x$ crystal

A. Zunger

Department of Theoretical Physics, Soreq Nuclear Research Centre, Yavne, Israel

Department of Chemistry, Tel Aviv University, Tel Aviv, Israel
(Received 7 January 1975)

A self-consistent LCAO tight binding calculation of the band structure of the one-dimensional $(SN)_x$ crystal is performed. Convergence of the band structure as a function of the interaction range and the number of translational irreducible representations that are allowed to interact (via the Hartree-Fock elements) as well as the SCF iteration cycle convergence are examined. The crystal is shown to possess a partially occupied valence band in accord with its experimentally established metallic behavior. Bond alternancy is investigated by examining the stability of the total energy with respect to conformational changes. The alternant structure is shown to be more stable than the equal-bond structure. Analysis of the charge distribution in the system reveals a low ionicity of the $S^{+\delta}N^{-\delta}$ bond ($\delta = 0.18e$) and points to the possibility of formation of cross bonds between nonbonded S-S pairs. The possibility of the occurrence of a Peierls instability was investigated by searching for a superlattice of model conformational distortions in the $(SN)_x$ chain that will both produce a gap around the Fermi level and lower the total Hartree-Fock crystal energy. Such an instability was not found, and the crystal was shown to behave like a metal for all the conformations studied.

I. INTRODUCTION

Recently, considerable interest has developed towards investigation of the electronic structure of highly anisotropic one-dimensional crystals that possess a metallic ground state such as the charge-transfer tetracyanoquinodimethan (TCNQ) salts,[1] mixed-valence Pt salts,[2] and polysulfur nitride $(SN)_x$.[3] Polysulfur nitride is the only known inorganic (one-dimensional) covalent crystal exhibiting metallic conductivity even at liquid helium termperatures.[3]

In early studies,[4] the electronic band structure of $(SN)_x$ was analyzed using a simple Huckel π-electron treatment and assuming an $-(N{=}S{=}N{-}S)$ structure with 3 π-electrons per (SN) unit. The energy of the lowest excitation was shown to approach zero as the bond lengths tend to equalize. The metallic behavior was thus attributed to low bond alternancy. This was consistent with early x-ray measurements[5] that suggested an equal-bond structure for $(SN)_x$. Recent electron diffraction studies[6,7] indicated that the crystal is made of infinite zigzag chains exhibiting strong bond alternancy (Fig. 1), the S=N and S–N bond lengths being 1.55 Å and 1.73 Å, respectively (double and single bond lengths in various SN compounds are 1.54 Å and 1.74 Å, respectively[8]). The crystal was shown to have a monoclinic space group $P2_1/C$ with the **b** axis oriented along the fiber direction and four SN units (two from each chain) per cell. The bending angles along the chain were determined to be approximately 108° and 119° at the nitrogen and the sulfur sites, respectively. The relations between the electronic structure and bond alternancy in $(AB)_n$ one-dimensional compounds has been the subject of many controversial studies.[9–13] Only limited studies have been made on the electrical and optical properties of $(SN)_x$. Thermoelectric measurements[3,14] have indicated a negative Seebeck coefficient, suggesting that the conductivity is primarily due to electrons. Compactions of $(SN)_x$ were shown[4] to exhibit a small activation energy of 0.02 eV in the temperature dependence of the conductivity, while crystals of $(SN)_x$ were shown to behave like a metal down to 4.2 °K.[3] The electrical conductivity was shown to increase rapidly, with pressure approaching a constant value at about 20 kbar.[4] Thermal conductance was shown to be 18 times larger than in polyethylene and approximately 1 order of magnitude larger than in most insulating molecular crystals.[14] The absorption spectrum of a deposited film of the polymer shows three transitions: at 0.02, 1.77, and 4–6 eV.[4]

In this paper we present a self-consistent LCAO (linear combination of atomic orbitals) band structure of the one-dimensional $(SN)_x$ crystal. We use both the experimental alternant crystal structure[6,7] and a model nonalternant structure. The crystal is shown to possess a partly occupied band in the ground state, in agreement with its metallic properties. Structure optimization calculations indicate that the alternant conformation is more stable than the equal-bond structure. Problems regarding the convergence of K-space sums, direct lattice sums, and SCF (self-consistent field) iteration cycles are discussed. Owing to the complexity in calculating all matrix elements by *ab initio* methods, semiempirical LCAO schemes are introduced to facilitate computations.

II. METHOD OF CALCULATION

The SN molecule is an open-shell structure consisting of 11 valence electrons. Since the crystal as a whole is nonparamagnetic, behaving as a closed-shell system, we adopt a single-determinant formalism restricting ourselves to the $(SN)_x$ structure for even values of x. We thus use an even number of h' molecules per unit cell, and at the end of the calculation the band structure will be analyzed according to the wave vectors K spanning the simple irreducible Brillouin zone consisting of a smaller number of SN molecules per unit cell. Throughout the calculations, h' will be taken as 2, 4, and 6, and the eigenvalue spectrum will be displayed for the primitive cell containing one SN unit. At the convergence limit of the calculation, the results obtained for different h' values should be the same. [For example, doubling the number of SN units results in a Brillouin zone that is smaller by a factor of 2 and contains twice as many bands. Since at the edges of the new Brillouin zone each pair of bands is degenerate (no gaps) due to

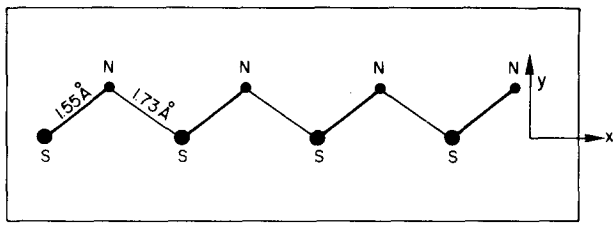

FIG. 1. Crystal structure of a one-dimensional alternant $(SN)_x$ crystal.

the one-dimensional group character, one can display these bands in the primitive Brillouin zone (one molecule per cell) without loss of information.] Bloch functions $\Phi_\mu^\alpha(\mathbf{K}, \mathbf{r})$ for the α sublattice and the μth atomic orbital $\chi_\mu(\mathbf{r}-\mathbf{R}_n-\mathbf{d}_\alpha)$ are constructed as

$$\Phi_\mu^\alpha(\mathbf{K}, \mathbf{r}) = N^{-1/2}\sum_{n=1}^{N} e^{i\mathbf{K}\cdot\mathbf{R}_n}\,\chi_\mu(\mathbf{r}-\mathbf{R}_n-\mathbf{d}_\alpha), \tag{1}$$

where $\mathbf{R}_n$ denotes the position of unit cell n, $\mathbf{d}_\alpha$ denotes the coordinates of the internal position of the atom belonging to sublattice $\alpha(\alpha = 1, 2\ldots, h$ for the diatomic molecules $h = 2h')$, and N indicates the number of unit cells. We employ σ_α atomic functions on each site α ($2s$ and $2p$ for nitrogen and $3s$, $3p$, or $3s$, $3p$, $3d$ for sulfur). Crystal orbitals belonging to the jth representation are generated by performing linear combinations of the Bloch functions, yielding

$$\psi_j(\mathbf{K}, \mathbf{r}) = \sum_{\mu=1}^{\sigma}\sum_{\alpha=1}^{h} C_{\mu j}^{\alpha}(\mathbf{K})\,\Phi_\mu^\alpha(\mathbf{K}, \mathbf{r}), \tag{2}$$

where σ denotes $\sum_\alpha \sigma_\alpha$. The secular equations yielded by applying the variational principle are given by

$$\sum_{\mu=1}^{\sigma}\sum_{\alpha=1}^{h}\left[F_{\mu\nu}^{\alpha\beta}(\mathbf{K}) - S_{\mu\nu}^{\alpha\beta}(\mathbf{K})\,\epsilon_j(\mathbf{K})\right]C_{\mu j}^{\alpha}(\mathbf{K}) = 0 \tag{3}$$

and define the band structure $\epsilon_j(\mathbf{K})$ for each band j. The matrix elements are given by

$$F_{\mu\nu}^{\alpha\beta}(\mathbf{K}) = \sum_n e^{i\mathbf{K}\cdot\mathbf{R}_n}\langle\chi_\mu(\mathbf{r}-\mathbf{d}_\alpha)|\,\hat{F}\,|\chi_\nu(\mathbf{r}-\mathbf{R}_n-\mathbf{d}_\beta)\rangle$$

$$\equiv \sum_n e^{i\mathbf{K}\mathbf{R}_n} F_{\mu\nu}^{\alpha\beta}(o, n), \tag{4a}$$

$$S_{\mu\nu}^{\alpha\beta}(\mathbf{K}) = \sum_n e^{i\mathbf{K}\cdot\mathbf{R}_n}\langle\chi_\mu(\mathbf{r}-\mathbf{d}_\alpha)|\chi_\nu(\mathbf{r}-\mathbf{R}_n-\mathbf{d}_\beta)\rangle$$

$$\equiv \sum_n e^{i\mathbf{K}\cdot\mathbf{R}_n} S_{\mu\nu}^{\alpha\beta}(o, n), \tag{4b}$$

where $\hat{F}$ denotes the Hartree–Fock operator and the reference unit cell is placed at the origin of the axis system. $S_{\mu\nu}^{\alpha\beta}(o, n)$ denotes atomic matrix elements between orbital μ of atom α situated at $(\mathbf{R}_0+\mathbf{d}_\alpha) = \mathbf{d}_\alpha$ and orbital ν of atom β situated at $(\mathbf{R}_n+\mathbf{d}\beta)$. The matrix element $F_{\mu\nu}^{\alpha\beta}(o, n)$ is given by

$$F_{\mu\nu}^{\alpha\beta}(o, n) = H_{\mu\nu}^{\alpha\beta}(o, n) + \sum_{\mu'\nu' s t'} P_{\mu'\nu' s t}^{\alpha\beta}$$

$$\times\left[(\mu o, \nu n|\,\mu' s, \nu' t) - \tfrac{1}{2}(\mu o, \nu' t|\,\nu n, \mu' s)\right], \tag{5}$$

where $H_{\mu\nu}^{\alpha\beta}(o, n)$ is the matrix element of the core Hamiltonian,

$$H_{\mu\nu}^{\alpha\beta}(o, n) = \langle\chi_\mu(\mathbf{r}_1-\mathbf{R}_0-\mathbf{d}_\alpha)|\,-\tfrac{1}{2}\nabla_1^2$$

$$-\sum_a\sum_m \frac{Z_a}{|\mathbf{r}_1-\mathbf{d}_a-\mathbf{R}_m|}\,|\chi_\nu(\mathbf{r}_1-\mathbf{R}_n-\mathbf{d}_\beta)\rangle, \tag{6}$$

and Z_a denotes the core-charge of atom a. $(\mu n, \gamma m\,|\,\mu' s\lambda' t)$ denotes the two-electron term

$$(\mu n, \lambda m\,|\,\mu' s, \lambda' t) = \langle\chi_\mu(\mathbf{r}_1-\mathbf{R}_n)\chi_\lambda(\mathbf{r}_1-\mathbf{R}_m)\,|\,\frac{1}{r_{12}}\,|\,\chi_{\mu'}(\mathbf{r}_2-\mathbf{R}_s)\chi_{\lambda'}(\mathbf{r}_2-\mathbf{R}_t)\rangle \tag{7}$$

and $P_{\mu'\nu' st}^{\alpha\beta}$ is the integral over the occupied part of the Brillouin zone (BZ) of the wave vector dependent bond-charge density matrix $P_{\mu'\nu'}^{\alpha\beta}(\mathbf{K})$:

$$P_{\mu'\nu' st}^{\alpha\beta} = \int_{\mathrm{BZ}_{oc}} d^3\mathbf{K}\,P_{\mu'\nu'}^{\alpha\beta}(\mathbf{K})e^{i\mathbf{K}(\mathbf{R}_s-\mathbf{R}_t)} \equiv P_{\mu'\nu'}^{\alpha\beta}(s-t), \tag{8}$$

where the notation of the BZ_{oc} integration volume implies an integration over the first BZ for the fully occupied bands and up to the Fermi momentum $\mathbf{K}_F$ for partially occupied bands. The wave vector dependent bond-charge matrix has elements given by

$$P_{\mu'\nu'}^{\alpha\beta}(\mathbf{K}) = \sum_j^{\sigma_{oc}} n_j\left[C_{\mu' j}^{\alpha}(\mathbf{K})\right]^*\left[C_{\nu' j}^{\beta}(\mathbf{K})\right]; \tag{9}$$

σ_{oc} denotes the number of bands that are occupied in the ground state, and n_j denotes the occupancy number for band j.

It is evident that owing to the explicit two-electron terms appearing in Eq. (5), the element $F_{\mu\nu}^{\alpha\beta}(o,n)$ depends not only on the electrons occupying the orbitals $\chi_\mu(\mathbf{r}-\mathbf{d}_\alpha-\mathbf{R}_o)$ and $\chi_\nu(\mathbf{r}-\mathbf{d}_\beta-\mathbf{R}_n)$ but also on all states that occupy the σ_{oc} bands in the BZ. Employing explicit two-electron interaction elements necessitates therefore a self-consistent treatment in which one guesses the elements of the charge density matrix $P_{\mu'\nu'}^{\alpha\beta}(\mathbf{K})$ for a chosen $\mathbf{K}$ grid, computes $P_{\mu'\nu' st}^{\alpha\beta}$ from Eq. (8), and then the elements $F_{\mu\nu}^{\alpha\beta}(\mathbf{K}_p)$ and $S_{\mu\nu}^{\alpha\beta}(\mathbf{K}_p)$ for a series of values $\{\mathbf{K}_p\}$. Then Eq. (3) is solved for these $\mathbf{K}_p$ values and from the resulting expansion coefficients $\{C_{\mu j}^{\alpha}(\mathbf{K}_p)\}$ one recomputes the charge density elements. At each iteration cycle the number of occupied bands σ_{oc} and the wave vector $\mathbf{K}_F$ of the highest occupied state are determined by assigning electrons to the calculated bands in an ascending order. The iteration cycle is terminated when the band energies $\epsilon_j(\mathbf{K})$ in two successive iterations do not exceed a prescribed tolerance (10^{-5}au in our calculation) and when the charge density is stable to within $10^{-7}e$ between successive iterations.

The total ground state energy for a given configuration of nuclei is the sum of the electronic contribution E_{elec} and the nuclear contribution E_{nuc}:

$$E_{\mathrm{elec}} = \tfrac{1}{2}\sum_{\mu\nu\alpha n} P_{\mu\nu}^{o,\alpha}(n)\left[H_{\mu\nu}^{o,\alpha}(n) + F_{\mu\nu}^{o,\alpha}(n)\right], \tag{10}$$

$$E_{\mathrm{nuc}} = \sum_{a<b}\frac{Z_a Z_b}{|\mathbf{R}_a-\mathbf{R}_b|}. \tag{11}$$

Stability of given crystal structures towards conformational changes are examined by performing numerical derivatives of the total energy with respect to conformational coordinates.

The convergence problems that occur in this formalism are

(a) convergence of contributions of interaction and overlap elements [Eqs. 4(a) and 4(b)] of various unit cells with respect to an origin unit cell. Special care must be taken to preserve lattice symmetry for each interaction radius in order to avoid spurious energy gaps that arise if "unbalanced" sums are taken.[15] M_R interaction terms are summed on both sides of a given atomic site and the convergence of the results as a function of M_R is examined. The electrostatic contributions of the second term in Eq. (6) plus the nuclear repulsion terms in Eq. (11) were summed in all cases up to a constant range of 65 Å to avoid an oscillatory behavior of these sums.[16]

(b) convergence of the elements of the charge density matrix (Eq. 8) as a function of the **K** grid used to evaluate the integrated density. The convergence of these elements is examined as a function of the number M_K of evenly-distributed **K** points in the BZ.

(c) convergence of the SCF cycle in the solution of Eq. (13) with the elements that are given in Eqs. (5–9).

(d) stability of the band structure with respect to the addition of more basis functions to Eq. (2). Owing to computational difficulties, only the effect of adding 3*d* orbitals to the sulfur atoms is investigated.

In this computation scheme, the full exchange terms are used and no spherical averaging of the potential around atomic sites is necessary. A similar computation scheme was previously employed by Andre[17] and Delhalle and Andre[18] and worked out on polyene and polyethylene on the *ab initio* level. SCF–LCAO schemes based on Fourier expansion of the electron density[19,20] or on the muffin-tin potential[21] usually utilize local Slater exchange and heavily rely on the spherical character of the potential around atomic sites. Tight binding methods,[22,23] directly applied to molecular rather than atomic crystals, involve spherical averaging of the molecular charge density and usually neglect three and four center integrals. Atomic crystals have been treated within the rigorous Hartree–Fock scheme by Harris *et al.*[24] and by Kunz.[25]

In view of the difficulties in implementing the suggested scheme in practice, we adopt semiempirical LCAO methods for evaluating the molecular integrals $F_{\mu\nu}^{\alpha\beta}(o,n)$ in Eq. (4a). We choose to work with the SCF–LCAO CNDO[26] scheme (complete neglect of differential overlap). Some results are also given for the less rigorous extended Hückel (EXH)[27] scheme. The approximations made in these methods and their relation to the more rigorous Hartree–Fock–Roothaan method are well documented in the literature and the reader is referred to Refs. 26–30 for details. The standard parameters given in the original papers are adopted for both the CNDO/2 and EXH calculations. These are taken from atomic spectra and from properties of small molecules. When more experimental data on optical properties of $(SN)_x$ and similar binary solids become available, a better parametrization scheme could be adopted. Alternatively, the results of the band structure computed with these approximations could be used as a first guess in the more refined *ab initio* iteration cycle. The semiempirical CNDO and EXH methods have been previously used to calculate various electronic properties of carbon polymers[31–35] and boron–nitrogen solids.[36,37]

Applying the EXH and CNDO/2 methods to a single SN molecule, one obtains values for the internuclear equilibrium distance of 1.43 Å and 1.53 Å, respectively, compared with the experimentally estimated value of 1.495 Å.[4] The ionization potential is 9.45 eV in the EXH and 12.2 eV in the CNDO/2 method. These differences are sufficiently large to suggest that the band structure in the solid should be examined with both approximations to avoid erroneous conclusions.

III. RESULTS

The band structure of a planar $(SN)_x$ chain with R_{SN} distances of 1.73 and 1.55 Å alternately and the chain angles from Refs. 6 and 7 is shown in Fig. 2 as calculated by both the CNDO/2 method (including 2*s* and 2*p* orbitals on nitrogen and 3*s*, 3*p*, and 3*d* orbitals on sulfur) and by the EXH method (2*s*, 2*p* and 3*s*, 3*p* orbitals on nitrogen and sulfur, respectively). The energy eigenvalues corresponding to an isolated SN molecule, calculated by these methods, are also indicated. The band structure is obtained at the convergence limit of the direct lattice sums, **K** space sums, and the iterative SCF cycle in the case of the CNDO/2 calculations (see below). The results corresponding to $h' = 2$, 4, or 6 SN units per cell, when displayed according to the wave vector of the irreducible primitive BZ, are the same. The five lowest valence bands are fully occupied in the ground state, while the sixth band (π^* band), composed mainly of sulfur $3p_z$ and to some extent by nitrogen $2p_z$ orbitals, is

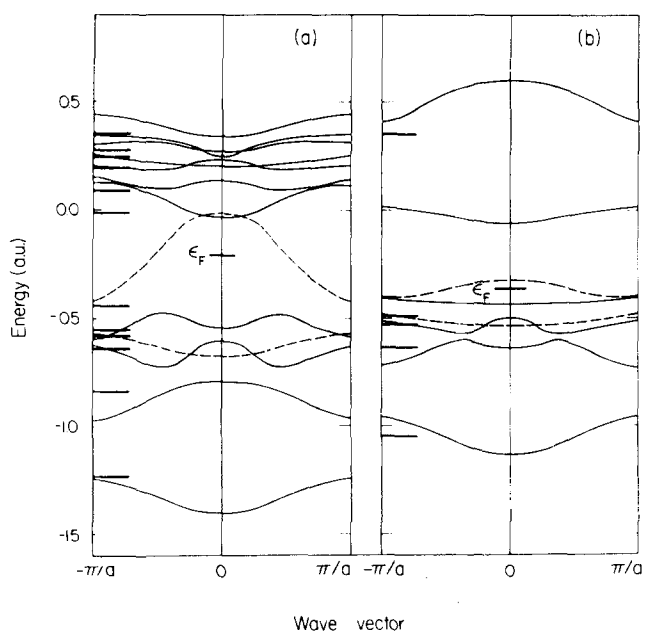

FIG. 2. Band structure of alternant nonlinear planar $(SN)_x$. Dotted lines indicate the π bands. SN distances are 1.73 Å and 1.55 Å alternately. The chain angles are taken from Refs. 6 and 7. (a) CNDO/2 calculation, (b) EXH calculation. The energy eigenvalues of the isolated SN molecule calculated by the two methods at the corresponding equilibrium distance for the molecule (CNDO/2: $R_{SN} = 1.53$ Å, EXH: $R_{SN} = 1.43$ Å) are indicated on the left.

only half occupied. The Fermi energy is 0.21 and 0.36 au for the CNDO and EXH calculations, respectively, and the Fermi momentum lies midway between the zone center and the zone edge. The calculated band structure thus predicts the true metallic character of the crystal. The lowest two valence bands are bonding and antibonding σ bands, respectively, mainly composed of the $2s$ and $3s$ Bloch functions. The π bands overlap strongly with the next σ bands that are mixtures of the in-plane Bloch functions ($2p_X^N$, $2p_Y^N$, $3p_X^S$, $3p_Y^S$, $3d_{X-Y}^S$, $3d_{XY}^S$, $2s^N$, and $3s^S$).

The general features of the band structure are similar in both the CNDO and EXH calculations, however, some quantitative differences are significant; e.g., the CNDO valence bandwidth (up to ϵ_F) is much larger (1.19 au) than the EXH bandwidth (0.77 au). Intraband excitations occurring in the partially occupied π^* band could give rise to the two lowest observed transitions at 0.02 and 1.77 eV,[4] while the lowest band-to-band transition calculated to be in the range of 5–8 eV could be tentatively assigned to the observed transition in the 4–6 eV region.[4]

While in the alternant *nonlinear* (bent) $(SN)_x$ chain there are two nondegenerate π bands (Fig. 2) extending along the axis perpendicular to the zigzag plane (Z direction in Fig. 1), in the alternant *linear* ($\theta = 180°$ in Fig. 1) chain there are two π bands, each doubly degenerate (Fig. 3) owing to the equivalence of the two spatial directions that are perpendicular to the chain axis (Z and Y directions, Fig. 1). The metallic behavior is still present since the number of SN units per unit cell, and thus the number of electrons that occupy the bands, is unchanged. Chapman *et al.*[4,14] treated the alternant nonlinear $(SN)_x$ system by a simple Hückel method considering only the π system. Since only the topology of the structure was taken into account, owing to neglect of overlap and retention of nearest neighbor interactions only, the *nonlinear* structure with three p_z electrons per SN unit and two such units per cell was assigned to have four π bands as in the *linear* alternant structure. This resulted in an incorrect nonconducting behavior for the crystal since the lowest bands were occupied by the 6 electrons, and thus a nonvanishing gap, proportional to the difference in the two resonant integrals (corresponding to the two S–N and S=N bond lengths), was obtained between the highest occupied and lowest vacant fourth band. Actually, in the nonlinear cases only two of the bands have π character, the other two bands transform like the in-plane $X-Y$ irreducible representations and thus mix with the $2s$ and $3s$ orbitals to form the σ bands. The two π bands are populated by the three π electrons per SN unit and indeed give rise to the true metallic behavior, as indicated by Walatka *et al.*[3]

The band structure of the linear $(SN)_x$ chain is shown in Fig. 3 for both CNDO and EXH calculations. The general features are similar to those of the nonlinear case (Fig. 2), except for the splitting of each of the former π bands into a π and σ band that strongly overlap. The energy difference between the two π bands at the edge of the BZ is proportional to the difference in the Coulomb integrals of sulfur and nitrogen and to twice

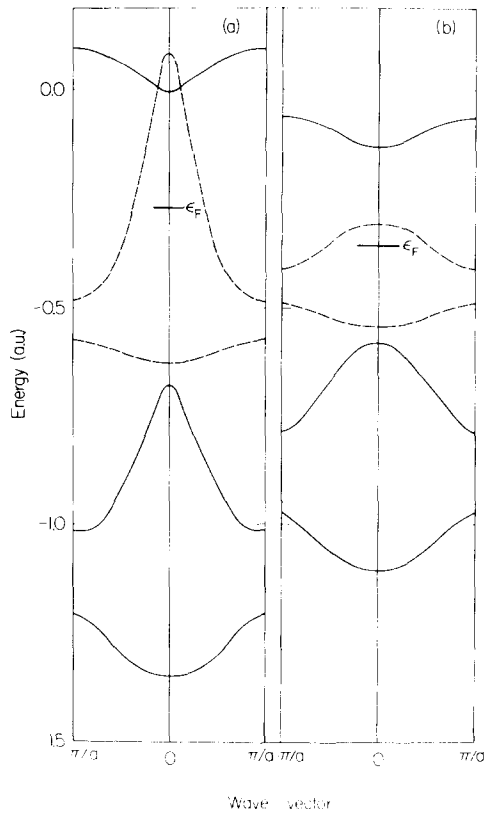

FIG. 3. Band structure of alternate linear $(SN)_x$. Dotted lines indicate the doubly degenerate π bands. SN distances are 1.73 Å and 1.55 Å alternately. The chain angle is $\theta = 180°$. (a) CNDO/2 calculation, (b) EXH calculation.

the difference in the resonance integrals of the short and long SN bonds. This gap corresponds to that calculated by Chapman *et al.*[4,14] but occurs between the two occupied states rather than between the occupied and vacant states. As the bond lengths tend to equalize in the nonlinear case, this gap approaches the constant limiting value of the Coulomb integral difference between the sulfur and the nitrogen. At this limit the π band edges are composed of pure p_z Bloch states of sulfur and nitrogen.

Owing to the more rigorous character of the CNDO/2 method, we proceed with it for discussing convergence properties. Tables I–III summarize the convergence checks performed. We first examine the effect of increasing the interaction radius (Table I) on band energies (the $\mathbf{K} = 0$ points were selected), binding energy per SN unit, net atomic charges, and diagonal Hartree–Fock matrix elements (the p_z elements are shown). It is evident that an increase in the interaction radius stabilizes all the valence bands and results in a net increase in binding energy. The conduction bands (not displayed in the table) show a pronounced destabilization upon increasing the interaction range due to their antibonding character. The lowest valence band, being composed of the more localized $2s_N$ and $3s_S$ orbitals, is only slightly affected by increasing the interaction radius, while the π^* band is more pronouncedly affected owing to the extended character of the p_Z, d_{Z^2}, and d_{XZ} orbitals. The diagonal p_Z Hartree–Fock elements change from the

TABLE I. Convergence of band energies at K = 0 (in order of increasing energy), binding energy per SN unit (relative to isolated atoms), atomic charges and diagonal Hartree–Fock matrix elements for p_z orbitals, as a function of the number of neighbors included in the lattice sums. Fifteen K points and a fully converged SCF cycle are used.

M_R	E_1^σ(a.u.)	E_2^σ(a.u.)	E_1^π(a.u.)	E_3^σ(a.u.)	E_4^σ(a.u.)	$E_2^{\pi*}$(a.u.)	Binding energy (a.u.)	$Q_S = -Q_N$ (e)	$F^{N,N}_{p_Z,p_Z}$	$F^{S,S}_{p_Z,p_Z}$
3	−1.334	−0.770	−0.649	−0.597	−0.531	+0.064	−0.641	0.101	−0.330	−0.225
5	−1.381	−0.781	−0.650	−0.601	−0.547	+0.021	−0.653	0.161	−0.300	−0.285
7	−1.383	−0.797	−0.658	−0.605	−0.549	−0.023	−0.699	0.185	−0.284	−0.375
9	−1.390	−0.799	−0.665	−0.609	−0.549	−0.016	−0.702	0.186	−0.274	−0.375
10	−1.390	−0.799	−0.666	−0.609	−0.549	−0.016	−0.702	0.186	−0.273	−0.376

isolated atom values of −0.21 and −0.34 au for sulfur and nitrogen, respectively, to −0.38 and −0.27 au, in the converged results. This is accompanied by a net flow of charge from sulfur to nitrogen. The effect of increasing the number of translational irreducible representations that are allowed to interact via the $F^{\alpha\beta}_{\mu\nu}(0, n)$ elements (Table II) are similar to the interaction radius effects. The effect of self-consistency (Table III) on the band energies is opposite to both lattice sum and K-sum effects. The one-electron band energies are destabilized after self-consistency is achieved (although the binding energy increases). Owing to these contrasting trends of the various convergences, one should treat all the convergence problems listed in Sec. II simultaneously before the results are accepted.

A separate calculation at the CNDO level, without the inclusion of the extravalence 3d orbitals on the sulfur, indicated that the effect of the 3d orbitals is to increase the dispersion of the π^* band, due to mixing of p_Z orbitals with $3d_{XZ}$ and $3d_{YZ}$ orbitals, resulting in a higher Fermi energy. The lowest π band contains only a small admixture of 3d orbitals, while the conduction π^* orbitals exhibit large 3d character. The binding energy increases by some 18% upon introducing the 3d orbitals while almost all one-electron occupied bands are destabilized in energy. These opposite trends could be present in an Hartree–Fock scheme, in which, contrary to the one-electron effective Hamiltonian schemes, the total energy is not just the sum of the band eigenvalues for all occupied states but also contains the core-Hamiltonian terms [Eqs. (10), (11)]. Similar effects were observed in the sulfur-bearing molecules H_2S, H_2SO, and H_2SO_2 when Hartree–Fock calculations were performed with and without sulfur 3d orbitals.[38]

The partial and net atomic charges of $(SN)_x$ are calculated by applying the Mulliken population analysis to the wavefunctions. The results are shown on Table IV. A net negative charge is accumulated on the nitrogen in accordance with its greater electronegativity. EXH results seem to overestimate significantly the ionicity of the structure. The tendency of the non-self-consistent EXH scheme to overestimate the charge transfer between atoms of different electronegativity has been previously discussed in detail.[28,29] CNDO charges are much more reliable and will be considered here. It is seen by inspection of Table IV that the 3d orbitals of sulfur are appreciably populated in the $(SN)_x$ structure (by almost 1e), the main contributions arising from 3d orbitals that have components along the chain axis (X direction in our calculation). The net atomic charges on sulfur and nitrogen (0.186 e and −0.186 e, respectively) imply low ionicity of the structure. The large values of the p_Z sulfur–sulfur bond order for the nonbonded nearest sulfur pair ($P^{S,S}_{p_Z,p_Z} = 0.326$) and the sulfur–nitrogen p_Z bond order (0.476 for the short S=N bond and 0.399 for the larger S–N bond) imply the existence of considerable cross linking in the chain. The effect of introducing sulfur 3d orbitals on the atomic charges is to induce a charge transfer of about 0.2 e from the more electronegative nitrogen atom to the sulfur, thus reducing the ionicity of the structure. Similar trends were observed in calculations of sulfur-containing small molecules.[38] The low interatomic charge transfer introduced by the inclusion of the 3d orbitals suggests that EXH results will still exhibit charge overestimation even if 3d orbitals will be included.

We next examine the stability of the nonalternant structure against bond alternation. For this purpose we compute the total energy per SN unit $E_{\text{tot}}(b, b)$ of a $(SN)_x$ structure with equal bonds of length b and for the structure in which the bond lengths differ by Δ: $E_{\text{tot}}(b, b-\Delta)$. We numerically approximate the derivative $\partial E_{\text{tot}}/\partial\Delta$ by using

TABLE II. Covergence of band energies at K = 0, binding energies, atomic charges and diagonal Hartree–Fock matrix elements as a function of the number M_K of the evenly distributed K points used. Ten neighbors and a fully convergent SCF cycle are used.

M_K	E_1^σ(a.u.)	E_2^σ(a.u.)	E_1^π(a.u.)	E_3^σ(a.u.)	E_4^σ(a.u.)	$E_2^{\pi*}$(a.u.)	Binding energy (a.u.)	$Q_S = -Q_N$ (e)	$F^{N,N}_{p_Z,p_Z}$ (a.u.)	$F^{S,S}_{p_Z,p_Z}$ (a.u.)
1	−1.371	−0.714	−0.660	−0.599	−0.535	−0.001	−0.695	0.110	−0.300	−0.341
5	−1.383	−0.745	−0.665	−0.607	−0.541	−0.010	−0.701	0.179	−0.285	−0.361
10	−1.385	−0.701	−0.666	−0.609	−0.548	−0.015	−0.702	0.186	−0.275	−0.371
15	−1.390	−0.799	−0.666	−0.609	−0.549	−0.016	−0.702	0.186	−0.273	−0.376

TABLE III. Band energies at K = 0, binding energy, atomic charges and diagonal Hartree-Fock matrix elements for uniterated and iterated results. Ten neighbors and 15 translational irreducible representations are allowed to interact.

	E_1^g(a.u.)	E_2^g(a.u.)	E_1^u(a.u.)	E_3^g(a.u.)	E_4^g(a.u.)	E_2^{u*}(a.u.)	Binding energy (a.u.)	$Q_S = -Q_N$ (e)	$F^{N,N}_{p_Z,p_Z}$ (a.u.)	$F^{S,S}_{p_Z,p_Z}$ (a.u.)
No SCF iterations	−1.406	−0.800	−0.680	−0.628	−0.556	−0.031	−0.680	0.279	−0.332	−0.347
SCF iterations	−1.390	−0.799	−0.666	−0.609	−0.549	−0.016	−0.702	0.186	−0.273	−0.376

$$\left[\frac{\partial E_{\text{tot}}}{\partial \Delta}\right]_b \cong [E_{\text{tot}}(b, b) - E_{\text{tot}}(b, b-\Delta)]/\Delta. \quad (12)$$

We have computed $[\partial E_{\text{tot}}/\partial\Delta]_b$ for the range $1.8\ \text{Å} \geq b \geq 1.5\ \text{Å}$. It is observed that for $b > 1.57$ Å the derivative is negative, suggesting an instability of the equal bond structure ($\Delta = 0$) with respect to bond alternation. The minimum energy structure for $\Delta = 0$ was calculated to be with $b \equiv R_{SN} = 1.57 \pm 0.02$ Å and a chain angle of 112° ± 2°. Complete optimization of the structure with respect to both bond distances and chain angles (allowing for deviation from a planar structure) would be desirable; however, it would be very time consuming to implement in practice.

Finally, we investigated the possibility of observing a Peirels instability in the pseudo-one-dimensional conductor.[39,40] This is done by searching a superlattice of conformational displacements in the $(SN)_x$ structure that will simultaneously introduce a gap in the partially occupied band around ϵ_F and lower the total crystal energy. It should be noted that in the Hartree–Fock formalism a lowering of a particular energy band is not always accompanied by a stabilization of the total crystal energy since the latter is not simply a sum of all energy eigenvalues of the occupied bands as it is in the simplified effective Hamiltonian calculation schemes. Since the Fermi momentum in the band structure of the regular $(SN)_x$ chain lies midway between the zone edge and the zone center (Fig. 2), we repeated the band structure calculation at the CNDO level, doubling the number of SN units in the crystal unit cell and introducing a parallel translational shift of every second SN molecule. This resulted in a small gap of about 0.1 eV between the newly formed occupied and vacant bands; however, the total energy was *increased* relative to the regular $(SN)_x$ structure. Similarly, other simple conformational changes introduced in a superlattice scheme, such as small rotations of a single superlattice of SN molecules along the chain axis leaving the second superlattice unchanged, did not produce a lowering of the crystal energy. Therefore, using a static model for Peirels instability, we were unsuccessful in finding a superlattice into which the crystal will transform as the temperature is lowered, thus changing to an insulating phase. It is also demonstrated that one should practice extreme caution when Peirels instabilities are to be deduced from band splitting without considering the accompanying changes in the total energy.

It should be mentioned that there exists yet another possibility of gap formation in the one-dimensional conductor, through neighboring correlation effects. Allowing for different spins for the different nth neighbor spatial functions (n being chosen for each crystal structure to permit a gap formation around the appropriate Fermi energy) in the band structure calculation results in a gap equation, formally analogous to that obtained in superconductivity theory.[16] This gap, reflecting the correlation between different spins in different orbitals, could be accompanied by energy lowering, thus producing a crystal instability. Investigations along this line with the "alternant molecular orbital" (AMO) formalism indeed confirmed the existence of a gap in a linear model of a hydrogen atom chain.[41,16]

IV. SUMMARY

Self-consistent LCAO tight-binding calculations for the band structure of $(SN)_x$ polymers have been performed The convergence limit of lattice sums, **K**-space sums and SCF iteration cycle is reached after introducing 7–10 interacting neighbors, 10–12 translational irreducible representations, and 8–12 iteration cycles. The simplification of the calculation of the molecular integrals, introduced via the self-consistent CNDO scheme, provide a practical calculation scheme. The non-self-consistent EXH method that has previously been shown to yield excellent results for carbon-containing polymers[17,18,31–35] fails in this case owing to the electronegativity difference between the atoms in the unit cell.

The $(SN)_x$ polymer is shown to exhibit a metallic character having a partially empty valence band. Bond alternancy stabilizes the system but does not affect the metallic properties. The sulfur 3d orbitals are significantly populated in this structure and mix considerably with the p_Z orbitals in forming the π bands. The charge distribution in the $(SN)_x$ system indicates very low ionicity and points to the possibility of formation of cross bonds

TABLE IV. Orbital and net atomic charges of the $(SN)_x$ crystal.

	CNDO/2		EXH	
Orbital	q_S	q_N	q_S	q_N
s	1.824	1.549	1.433	1.130
p_X	0.714	1.169	0.527	1.268
p_Y	0.784	1.315	1.406	1.736
p_Z	1.497	1.153	1.364	1.636
d_{Z2}	0.098			
d_{XZ}	0.308			
d_{YZ}	0.044			
d_{X-Y}	0.326			
d_{XY}	0.219			
Q_{net}	0.186	−0.186	1.270	−1.270

between neighboring sulfur and nonbonded sulfur–nitrogen atoms. A search for a Peirels instability, by investigating a superlattice of model conformational distortions that will simultaneously produce a band gap and lower the total energy, was unsuccessful, and the calculations reveal a metallic behavior for all investigated structures.

The role of interchain coupling, introduced by allowing different $(SN)_x$ chains to interact, as well as a more rigorous *ab initio* band structure calculation, would be the next steps to be undertaken to further elucidate the electronic properties of $(SN)_x$ crystals.

[1]I. F. Shchegolev, Phys. Status Solidi A 12, 9 (1972).
[2]H. R. Zeller, in *Festkörperproblems*, edited by H. J. Queisser (Pergamon, New York, 1973), Vol. 13.
[3]V. V. Walatka, M. M. Labes, and J. H. Perlstein, Phys. Rev. Lett. 31, 1139 (1973).
[4]D. Chapman, R. J. Warn, A. G. Fitzgerald, and A. D. Joffe, Trans. Faraday. Soc. 60, 294 (1964).
[5]M. Goehring, Quart. Rev. Chem. Soc. 10, 437 (1950); M. Goehring and D. Voigt, Z. Anorg. Allg. Chem. 785, 181 (1950).
[6]M. Boudeulle and P. Michel, Acta Crystallogr. A 28, S199 (1972).
[7]M. Boudeulle, M. A. Douillard, P. Michel, and G. Vallet, C. R. Acad. Sci. C 272, 2137 (1971).
[8]See papers in *Sulfur Research Trends*, edited by R. F. Gould, Advances in Chemistry Series No. 110 (American Chemical Society, Washington, D.C., 1972).
[9]D. W. Davies, Nature (Lond.) 194, 82 (1962).
[10]C. W. Haigh and L. Salem, Nature (Lond.) 196, 1307 (1962).
[11]D. Chapman and A. D. McLachlan, Trans. Faraday Soc. 60, 2671 (1964).
[12]Y. Ooshika, J. Phys. Soc. Jpn. 12, 1246 (1957).
[13]J. M. Andre and G. Leroy, (a) Int. J. Quantum Chem. 5, 557 (1971) and (b) Chem. Phys. Lett. 5, 71 (1970).
[14]P. L. Kronick, H. Kaye, E. F. Chapman, S. B. Mainthia, and M. M. Labes, J. Chem. Phys. 36, 2235 (1962).
[15]F. O'Shea and D. P. Santry, Chem. Phys. Lett. 25, 164 (1974).
[16]K. F. Berggron and F. Martino, Phys. Rev. 184, 484 (1969).
[17]J. M. Andre, J. Chem. Phys. 50, 1536 (1969).
[18]J. Delhalle, J. M. Andre, S. Delhalle, J. J. Pireaux, R. Caudano, and J. J. Verbist, J. Chem. Phys. 60, 545 (1974).
[19]J. Callaway and J. L. Fry, in *Computational Methods in Band Theory*, edited by P. M. Marcus, J. F. Janak, and A. R. Williams (Plenum, New York, 1971), p. 512.
[20]D. M. Dorst and J. L. Fry, Phys. Rev. B 5, 684 (1972).
[21]J. E. Falk and B. J. Fleming, J. Phys. C 6, 2954 (1973).
[22]F. Bassani, L. Pretronero, and R. Resta, J. Phys. C 6, 2133 (1973).
[23]G. P. Parravicini and L. Resca, Phys. Rev. B 8, 3009 (1973).
[24]F. E. Harris and H. J. Monkhorst, Solid State Commun. 9, 1449 (1971).
[25]A. B. Kunz and D. J. Mickish, Phys. Rev. B 8, 779 (1973).
[26]J. A. Pople and D. L. Beveridge, *Approximate MO Theory* (McGraw Hill, New York, 1970).
[27]R. Hoffman, J. Chem. Phys. 39, 1397 (1963).
[28]G. Blyholder and C. A. Coulson, Theor. Chim. Acta 10, 316 (1968).
[29]L. C. Allen and J. D. Russel, J. Chem. Phys. 46, 1029 (1967).
[30]T. L. Gilbert, in *Molecular Orbits in Chemistry, Physics and Biology*, edited by O. Sinanŏglu (Yale U. P., New Haven, 1964), p. 405.
[31]K. Morokuma, J. Chem. Phys. 54, 962 (1971).
[32]D. L. Beveridge, I. Jano, and J. Ladik, J. Chem. Phys. 56, 4744 (1972).
[33]J. Ladik and K. Appel, J. Chem. Phys. 40, 2470 (1964).
[34]W. L. McCubbin and R. Manne, Chem. Phys. Lett. 2, 230 (1968).
[35]S. O'Shea and D. P. Santry, J. Chem. Phys. 54, 2667 (1971).
[36]D. R. Armstrong, B. J. McAloon, and P. G. Perkins, Trans. Faraday Soc. 69, 968 (1973).
[37]A. Zunger, J. Phys. C 7, 76 (1974); 7, 96 (1974).
[38]J. R. Van Wazer and I. Absar, in *Sulfur Research Trends*, edited by R. F. Gould, Advances in Chemistry Series No. 110 (American Chemical Society, Washington, D.C., 1972), p. 20.
[39]R. E. Peirels, *Quantum Theory of Solids* (Oxford, London, 1956), p. 108.
[40]B. Renker, H. Rietschel, L. Pintschovius, W. Glaser, P. Bruesch, D. Kuse, and M. J. Rice, Phys. Rev. Lett. 30, 1144 (1973).
[41]J. L. Calais, Ark. Fys. 28, 511 (1965).